JSAE 20119150
SAE 2011-01-1893

Validation and Application of a New 0D Flame/Wall Interaction Sub Model for SI Engines

Maria Rivas
Renault, France

Pascal Higelin, Christian Caillol
PRISME, Orleans France

Olivier Sename, Emmanuel Witrant
GIPSA Lab, Grenoble France

Vincent Talon
Renault, France

ABSTRACT

To improve the prediction of the combustion processes in spark ignition engines, a 0D flame/wall interaction submodel has been developed. A two-zones combustion model is implemented and the designed submodel for the flame/wall interaction is included. The flame/wall interaction phenomenon is conceived as a dimensionless function multiplying the burning rate equation. The submodel considers the cylinder shape and the flame surface that spreads inside the combustion chamber. The designed function represents the influence of the cylinder walls while the flame surface propagates across the cylinder. To determine the validity of the combustion model and the flame/wall interaction submodel, the system was tested using the available measurements on a 2 liter SI engine. The model was validated by comparing simulated cylinder pressure and energy release rate with measurements. A good agreement between the implemented model and the measurements was obtained.

INTRODUCTION

Modern automobile engines must fulfill challenging conditions in terms of efficiency and pollutant emissions while keeping performance. The answer to these constraints has been the development of new modes of combustion and the inclusion of mechanical devices such as turbochargers, variable valve timing (VVT) and exhaust gas recirculation (EGR). These new developments improve dramatically the engines performance, but their inclusion also results in a less predictable combustion, which might alter the proper functionality of the exhaust treatment systems. Studies in this area have coincided with the fact that in order to maintain the performance of these systems, a more accurate prediction of the phenomenological combustion modeling is essential.

In the case of SI engines, several combustion models have been proposed, in most of them, the heat release is modeled by the classical turbulent premixed flame propagation. [1] provides a summary of different common combustion models. The main differences between the different propositions are associated with the modeling of the wrinkling phenomenon of the flame surface. Two different models were studied in this work: coherent flame model (CFM) and Fractal Combustion Model.

In [2], a 3D CFM model is developed. It describes the rate of fuel consumption per unit volume by the product of the flame surface density and the local speed at which it consumes the mixture. This model was reduced to 0D in [3]. In [4], [5] and [6], different fractal combustion models are proposed and the most relevant elements to characterize the fractal representation of the burning rate are developed. In this work, the fractal combustion model from [5] and its complement from [7] are implemented.

The previous 0D models mostly focus on the laminar characteristics and on the wrinkling phenomena of a free developing flame, but they lack a suitable approximation of the wrinkling phenomenon when the flame reaches the cylinder walls. The cylinder wall is a barrier that limits the fuel mobility. Besides, the wall temperature is colder when compared to the gases temperature, which decreases the gases expansion. These phenomena reduce the burning rate. This behavior might depend on the engine intake geometry, the combustion chamber geometry and the operating conditions [8]. Such a flame-wall interaction is an essential issue in accurately modeling the combustion process.

In this paper, a new model that takes into account the impact of the cylinder walls in the burning rate is proposed. This approach is based on the flame surface distribution with respect to the combustion chamber and the assumed linear decay during the flame-wall interaction. A well defined geometric model of the combustion chamber is designed in order to have more realistic results. The model is included in a 0D two-zones combustion model and can be included in several combustion schemes since it is conceived as a dimensionless function multiplying the burning rate equation. The model is tested taking as reference the available measurements on a 2 liters engine. It is validated with the data fit of the cylinder pressure and the energy release during the combustion.

In this paper the two zones thermodynamical model and the combustion model are described. A previous model to represent the combustion close to the walls is presented, this approximation was used before moving to the current approximation and will help to understand the improvements obtained with the main result of this work. Subsequently, the submodel to take into account the impact of the cylinder walls in the burning rate is illustrated, this model constitutes the main result of this work. Finally, comparison with experimental results are presented.

TWO ZONES THERMODYNAMICAL MODEL

There are some assumptions in the spark-ignition engine combustion process that permits a representation of this process with a two zones approximation [9]. Those assumptions are:

- the fuel, air and residual gases charge is uniformly premixed;
- the volume occupied by the reaction is small in comparison with the clearance volume, which means that the flame is a thin reaction sheet that becomes wrinkled as it develops.

Under these assumptions it can be assumed that the cylinder volume is divided into two zones: the burned gases and the unburned gases zones separated by the reaction layer. Each zone is defined by its mean thermodynamics properties and the specific heat of each gas component changes according to the JANAF thermodynamic properties table [10].

Both zones are assumed to have the same uniform in-cylinder pressure. The thermodynamical model describes the energy balance inside the combustion chamber. Each zone is considered as a separate open system. The mass flow rate into each zone is deduced from a balance equation corresponding to the mass transfer through intake and exhaust valves. The mass transfer between the two zones is modeled by the two zones combustion model detailed next.

The energy equation for each zone is inferred from [11] as:

$$dU_i = \delta Q_{th,i} - pdV_i + \Big(\sum_j h_j dm_j\Big)_i \tag{1}$$

where the subscript i denotes the zone: $i = b$ for burned gases or $i = u$ for unburned gases, U_i is the internal energy of the cylinder gas mixture, $\delta Q_{th,i}$ expresses the heat transfer of the cylinder contents to the surroundings, pdV_i corresponds to the work delivered by the piston, $\sum_j h_j dm_j$ is the total energy flowing into or out of the zone i and h_i is the specific enthalpy of each zone.

The left hand side of (1) can be written as:

$$dU_i = u_i dm_i + m_i \sum_k u_{i,k} dY_{i,k} + m_i c_{v,i} dT_i \tag{2}$$

where $u_{i,k}$ is the internal energy of species k in the zone i and u_i corresponds to the internal energy of the whole mixture, $Y_{i,k}$ corresponds to the mass fraction of species k in the zone i. m_i is the total mass in zone i and T_i corresponds to the temperature of the mixture in the zone i.

Solving (1) and (2) for dT, two ordinary differential equations are implemented as governing equations for the system temperatures dynamics:

$$dT_u = \frac{1}{m_u c_{p,u}}\left(V_u dp - \delta Q_{w,u} - h_u dm_u + \left(\sum_j h_j dm_j\right)_u\right) \tag{3}$$

$$dT_b = \frac{1}{m_b c_{p,b}}\left(V_b dp - \delta Q_{w,b} - h_b dm_b + \left(\sum_j h_j dm_j\right)_b\right) \tag{4}$$

where V_u is the unburned gases volume, V_b is the burned gases volume. The cylinder charge is supposed to be premixed and homogeneous, which implies that $dY_{i,k} = 0$.

The term $\delta Q_{th,i}$ has been replaced by $-\delta Q_{w,i}$ because the heat transfers to the surroundings are considered as heat losses into the cylinder walls. The heat losses from the gases in the combustion chamber to the cylinder walls are given by:

$$\delta Q_{w,i} = h_c A_{w,i}(T_i - T_w) \tag{5}$$

where $A_{w,i}$ is the wall transfer area for each zone, $T_i - T_w$ is the temperature difference between the gases (burned or unburned) and the cylinder walls and h_c is the heat transfer coefficient computed from Woschni's equation [12].

The volume V_i in each zone is defined by the algebraic relation:

$$V_b = \frac{m_b r_b T_b}{m_b r_b T_b + m_u r_u T_u} V_{cyl} \tag{6}$$

$$V_u = V_{cyl} - V_b \tag{7}$$

where r_i is the mixture specific gas constant in zone i and V_{cyl} is the cylinder volume. Finally, putting together equations (3) and (4) and solving for dp, the in-cylinder pressure dynamics is modeled as:

$$\begin{aligned} dp = \frac{1}{\frac{V_u}{\gamma_u} + \frac{V_b}{\gamma_b}} \Bigg\{ & \left(1 - \frac{1}{\gamma_u}\right) \delta Q_{w,u} + \left(1 - \frac{1}{\gamma_b}\right) \delta Q_{w,b} \\ & - pdV - \left(\frac{1}{\gamma_u} - 1\right) \left(\sum_j h_j dm_j\right)_u \\ & - \left(\frac{1}{\gamma_b} - 1\right) \left(\sum_j h_j dm_j\right)_b \\ & + dm_u \left(\frac{1}{\gamma_u} h_u - u_u\right) + dm_b \left(\frac{1}{\gamma_b} h_b - u_b\right) \Bigg\} \end{aligned} \tag{8}$$

COMBUSTION MODEL

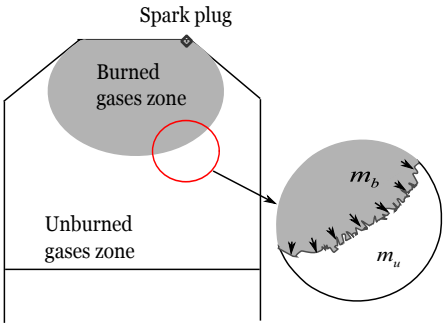

Figure 1: Two zones model scheme: the fresh gases are locally dragged to the wrinkled flame front at the laminar speed S_l

Recent combustion models are generally based on the flamelet assumption, where the combustion reaction is assumed to be fast enough so that the dominant effect of turbulence on the flame is to wrinkle the flame surface while the inner flame structure is not significantly altered by the turbulent flow field [13].Under these assumptions, the mass burning rate is proportional to the density of the unburned mixture ρ_u, to the turbulent flame speed S_t and to the laminar flame area A_l, considered as a spherical surface centered in the spark plug location, which implies that:

$$dm_b = \rho_u A_l S_t \tag{9}$$

After ignition, the flame surface propagates freely across the combustion chamber, the fresh gases reach the flame front at the laminar flame speed S_l and they get burned in a thin front layer. In Figure 1, a schematic view of the two zones is presented. The main idea of this model is to describe the burning rate of the fuel and the fresh air while they get burned in the combustion chamber.

The turbulent flame speed is defined as $S_t = S_l \Xi$, where S_l is the laminar speed of the flame, derived from experimental measurements in [14] as:

$$S_l = S_{L0} \left(\frac{T_u}{T_0}\right)^{\alpha} \left(\frac{p}{p_0}\right)^{\beta} (1 - 2.21 X_{egr}^{0.773}) \tag{10}$$

The parameters S_{L0}, α and β are characteristics of the fuel. In [15], specific data to characterize these parameters are given. For the study considered here:

$$\alpha = 2.4 - 0.271\phi^{3.51} \tag{11}$$

$$\beta = -0.357 + 0.14\phi^{2.77} \tag{12}$$

$$S_{L0} = \beta_m + \beta_\phi (\phi - \phi_m)^2 \tag{13}$$

where $\beta_m = 30.5\, cm/s$, $\phi_m = -54.9\, cm/s$ and ϕ is the equivalence ratio of the mixture.

Ξ is the turbulent wrinkling coefficient; this factor represents the increase in the flame surface, $\Xi = A_t/A_l$, where A_t is the wrinkled turbulent flame surface. Thus, the burning rate of the fuel is expressed as:

$$dm_b = \rho_u A_l S_l \Xi \tag{14}$$

During the combustion process, the wrinkling coefficient Ξ increases the turbulent burning rate. At

the beginning of the combustion the flame surface is not wrinkled by turbulence, while the flame surface reaches a given radius, it is supposed to be laminar ($\Xi = 1$). Once the transition radius is reached, the wrinkles in the upper layer of the surface are significant and this phenomenon is taken into account by the wrinkling factor that multiplies the burning rate ($\Xi > 1$).

In the literature, different ways to model this wrinkling coefficient are proposed. In this work, a fractal theory based wrinkling coefficient developed in [5] was implemented. It is detailed in the next section.

FRACTAL THEORY BASED WRINKLING COEFFICIENT

Applying fractal geometry concepts to the modeling of the wrinkled flame front surfaces has shown to give suitable estimations of the turbulent speed [16]. In the fractal model, it is assumed that the wrinkling phenomenon may be represented by a fractal dimension D_3 for a range of length scales L_{min} and L_{max}. The wrinkling coefficient Ξ is expressed as:

$$\Xi = \left(\frac{L_{max}}{L_{min}}\right)^{D_3-2} \tag{15}$$

Substituting (15) in (14) gives:

$$dm_{b_{fractal}} = \rho_u A_l S_l \left(\frac{L_{max}}{L_{min}}\right)^{D_3-2} \tag{16}$$

The fractal dimension D_3 is a function of the turbulent flow behavior inside the chamber. For this model, a simple phenomenological 0D turbulence model from [17] is retained. It is presented at the end of this document in the appendix.

The Kolmogorov's scale L_k is chosen as the minimum wrinkling scale L_{min} [5]. The maximum wrinkling scale is a function of the flame radius times a calibration constant $L_{max} = c_r R_f$, where R_f is the mean flame radius of the flame spherical surface A_l. The fractal dimension D_3 depends on the turbulence intensity u' and the laminar flame speed S_l as [5]:

$$D_3 = \frac{2.35u' + 2.05S_l}{u' + S_l} \tag{17}$$

Note that the computation of this process is assumed to start at the end of the kernel initiation process. The fractal burning rate approximation is finally obtained as:

$$dm_{b_{fractal}} = \rho_u A_l S_l \left(\frac{c_r R_f}{L_k}\right)^{D_3-2} \tag{18}$$

FLAME SURFACE

In order to implement the combustion model a well defined design of the flame surface is necessary. The flame surface model is the basis for the combustion close to the walls model. To model the combustion chamber and the flame surface progressing inside it, the following parameters are taken into account:

- cylinder geometry (Bore, spark position, chamber height);
- piston height;
- burned gases volume during combustion.

With these parameters, a simplified geometric model of the combustion chamber is obtained. The values that define this model are stored in a data map. Following the same principle, a geometric spherical surface of the flame progressing inside the combustion chamber is designed as presented in Figure 2. The data map is inverted to obtain the flame radius and the flame surface as a function of the piston height and the burned gases volume.

The input parameters to define the flame surface evolving inside the combustion chamber are the piston height and the available volume. Using the surface geometrical model and the burned gases volume from the two zones model, the input parameters of the surface model map are extrapolated during the simulation in order to obtain a flame radius and a flame surface.

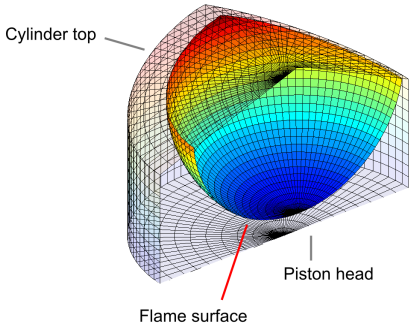

Figure 2: Scheme of the flame surface developing inside the combustion chamber

When the combustion takes place, the burned gases increase and the flame surface expands, occupying the available volume in the combustion chamber. This behavior results in changes in the burned gases density, but the burned gases volume

never decreases. In the flame surface model, the ratio between the volume of the burned gases and the available cylinder volume V_b/V_{cyl} is taken into account as an input parameter. The volumes ratio increases in time as a function of the piston height and the burned gases volume: it starts at zero at the beginning of the combustion and increases towards one, when the burned gases volume equals the available cylinder volume. This surface model is the basis to characterize the amount of flame that is close to the cylinder walls.

COMBUSTION MODEL WITH FLAME/WALLS INTERACTION

When the flame front approaches the cylinder wall, there is a deceleration of the burning rate because the boundary layer of the walls surface acts as a barrier that extinguishes the gases expansion and the relatively low temperature of the walls colds the gases. A considerable fraction of the unburned mixture actually burns in this combustion mode [18]. Consequently, the wrinkling coefficient Ξ as presented in the previous sections is valid when the flame surface propagates freely across the chamber, but the combustion close to the cylinder walls is not well represented.

Many studies have been performed in order to predict the flame-wall interaction. In [19], the flame-wall interaction is modeled by a semi-empirical expression, the Weller's approximation, but it lacks of information about its implementation. In [20] Weller's work is cited omitting the flame-wall interaction; it is replaced by a quenching law, where the burning rate near to the walls is estimated as a function of the mean burning rate and the mass fraction species (fresh gases and quenched gases). It is assumed that the quench distance is inversely proportional to the square root of the pressure. In this approximation it is not well established how to define the boundaries for the quenching zone and the estimation of the quenched gases fraction. Another approximation is proposed in [21], where the flame-wall interaction is related to the enthalpy close to the walls region, this model requires a third zone between the burned and unburned zones. In [22], a quenching coefficient is calculated measuring the length of the wrinkles in the vicinity of the piston. A linear decrease in the burning rate from a given distance to the cylinder walls was found. This result is used as an hypothesis for the final contributions of this work. This section is focused on the implementation of a submodel that represents the influence of the cylinder walls in the burning rate.

CHARACTERISTIC INTEGRAL LENGTH SCALE

A main issue to understand the flame/walls interaction is the condition where the flame surface is supposed to be influenced by the cylinder walls. As the mean flame surface is assumed to be spherical, when the flame radius reaches a given length from the cylinder walls, the influence can be considered.

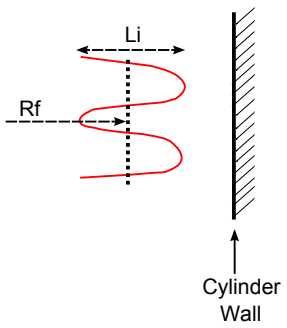

Figure 3: Scheme of the flame approaching to the cylinder walls and the distance to take into account the flame/wall interaction

In order to find the distance where the walls influence the combustion process, the fluid dynamics behavior of turbulent flows is considered. The turbulent behavior depends on the spatial distribution of the gases in the chamber and the influence of the piston movement. These characteristics are explained by the spatial and time scales of the eddy flows. The length scales are explained from 3D turbulence models, i.e [23], but 0D approximations are mainly represented by geometrical models or measurements. [24], [25] and [26] provide some estimations for the characteristic length scales .

The large scale eddies, characterized by the integral length scale L_i, represent the largest turbulent eddies occurring in a given geometry (refer to the Appendix for a more detailed explanation) as depicted in Figure 3. In this case, the integral scale seems to be a suitable reference to consider the walls influence. Thus, when the flame radius reaches a value such as $R_f > R_{cyl} - L_i/2$, the walls influence is considered.

GLOBAL APPROACH

In this section, a weighting term w that represents the transition between the turbulent combustion mode and the walls combustion mode similarly to [5] is implemented. w increases linearly with time: it models which one of the two combustion modes, fractal or near to walls, has more influence on the process. The resulting burned mass dynamics is:

$$dm_{b_{overall}} = (1-w)dm_{b_{fractal}} + wdm_{b_{walls}} \tag{19}$$

where w is given by:

$$w = 1 - \frac{m - m_b}{(m - m_b)_{tr}} \tag{20}$$

In [5], tr is the time when the transition between the turbulent combustion mode and the walls combustion

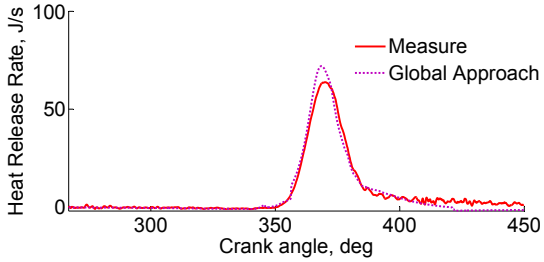

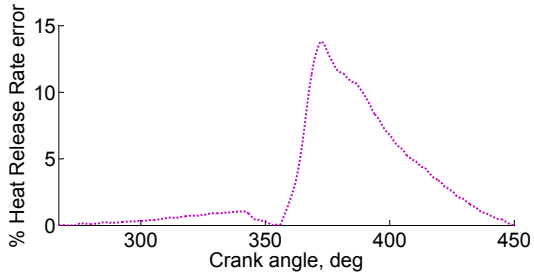

(a) Heat release rate

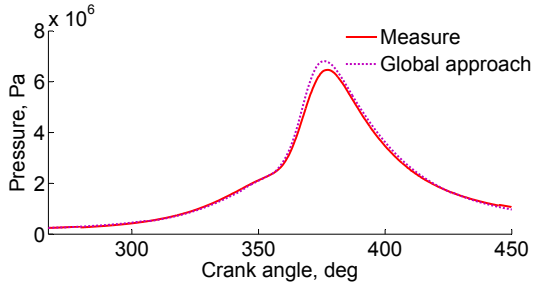

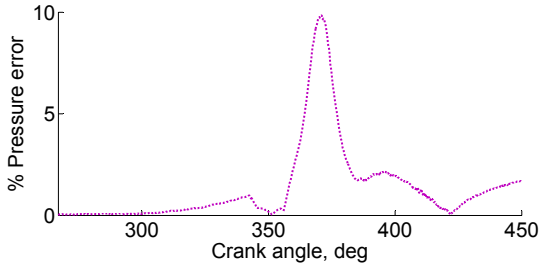

(b) Cylinder Pressure

Figure 4: Heat release rate and cylinder pressure for the burning rate model (19)

mode occurs. It is computed at a fixed distance from the cylinder walls, called the transition length, where the combustion model shifts from a fractal burning rate to a linear deceleration:

$$dm_{b_{walls}} = \frac{m - m_b}{\tau} \tag{21}$$

The characteristic time τ is computed in the transition length, thus the burning rate speed during the rest of the cycle is assumed to be equal to the one computed from the fractal mode at the transition time tr as:

$$\tau = \frac{(m - m_b)_{tr}}{dm_{b_{fractal}}} \tag{22}$$

Even if this approximation gives an acceptable result for the cylinder pressure computation, various concepts are questioned from this approximation:

- the unburned mass available in the combustion chamber $m - m_b$ is not necessarily close to the cylinder walls at a given time tr: the assumption of a linear decay of this mass is consequently not consistent with the model;
- the approximation for τ suggests that the burning rate when the flame gets close to the walls equals to the one derived in the fractal approximation, which is not accurate since the burning rate tends to be more similar to the one corresponding to a laminar flame [22] close to the walls. Even if w might supply the desired effect, it lacks a physical sense.
- the combustion chamber shape is not taken into account to consider the flame-wall interaction.

Figure 4 shows the system simulation using (19). In Figure 4a, it is possible to see that there is an overestimation in the heat release rate. This overestimation is reflected in the cylinder pressure, depicted in Figure 4b. In the figures, the crank angle is referenced from 0^o to 720^o for a complete cycle, starting in the admission stroke and the top dead center (TDC) is placed at 360^o. The test was performed at an engine speed of $N = 5250\,rpm$, and a brake mean effective pressure BMEP $= 11.4\,bar$.

Aiming to propose a more realistic approximation of the combustion process behavior close to the cylinder walls than the global approach, the cylinder shape and the flame surface distribution in the combustion chamber have to be taken into account. This allows to model in which proportion the cylinder wall affects the flame expansion inside the combustion chamber. A local approach of the flame-wall interaction has been modeled. This new approach complements the fractal combustion model introducing the flame-wall interaction during all the combustion phase instead of switching to a linear deceleration from a given moment of the combustion as the global approach has suggested. This new approach is exposed in the next subsection.

LOCAL APPROACH

As mentioned before, the burning rate during the combustion exhibits a deceleration when the flame surface is getting close to the cylinder walls. In order to model this behavior, the term Ψ is introduced in equation (14) as:

$$dm_{b_{overall}} = \rho_u A_l S_l \Xi \Psi \quad (23)$$

Differently from the global model (19) presented in the previous section, in the local approach, Ψ introduces a deceleration in the burning rate while taking into account the cylinder geometry and the burned gases volume in the combustion chamber. Moreover, Ψ does not switches from a combustion mode to another, but it proportionates a continuous calculation of the cylinder walls influence during the whole combustion process.

Two main aspects are taken into account to build Ψ: the distribution of the flame surface with respect to the cylinder walls and an extinction function to consider the influence of the wrinkling phenomenon depending on the distance of the flame surface to the cylinder walls.

Flame distribution with respect to the walls

Using the flame surface model exposed before, it is possible to compute the normal distance from the flame surface to the cylinder walls during combustion and express it as a fraction of flame surface. This distribution is a function of the flame radius and the piston height. This concept is presented in Figure 5, where A_t is the total flame surface and A_{di} is the flame surface in a given point which is at a distance d_i from the cylinder walls.

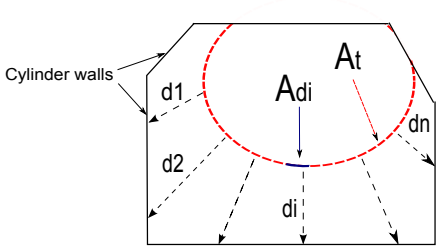

Figure 5: Flame surface distribution with respect to the cylinder walls distance.

The flame surface is divided in n parts. Each part is considered as tangential to the flame surface centered at a point. The distance between each one of these points and the cylinder walls, in the direction normal to the surface is calculated, resulting on a distribution of the flame surface with respect to the cylinder walls distance. With this distribution it is possible to compute the flame surface fraction at a given distance (i.e $(d_1, d_2, ...d_m)$), from the cylinder walls. The surface fraction in Figure 5 is computed as the sum of the area at a fixed normal distance from the flame surface to the cylinder walls divided by the total flame surface:

$$A_{f_{d_i}} = \frac{\sum_j A_{d_i,j}}{A_t} \quad (24)$$

where $A_{d_i,j}$ is the surface of all the j flame surface points at a distance d_i from the cylinder wall ($j < n$) and

$$A_t \approx \sum_i A_{d_i} \quad (25)$$

The flame surface fraction $A_{f_{d_i}}$ is calculated for a set of distances from the cylinder wall, which provides the map of flame surface distribution with respect to the cylinder walls distance. The map has as inputs the flame radius R_f, the piston height and the distance to take into account the walls influence d_i. The output is the flame surface fraction at a given distance d_i from the cylinder walls. In the simulation, the values of the two-zones model are used into the map to obtain the global distribution of the system. Figure 6 shows the obtained distribution with respect to the flame radius during simulation. As expected, when the flame radius is small, the flame surface fraction which reaches the cylinder walls is small. When the radius increases, the flame fraction tends to 1.

As presented before, the distance from the flame surface to the cylinder is $L_i/2$, to consider the influence of the walls. Figure 7 shows a simulation of the flame surface distribution with respect to the crank angle when the distance to the cylinder walls is below $L_i/2$. As it is expected, when the combustion has not started the flame fraction is null. Once the combustion starts, the flame wrinkles start to appear and the flame surface starts to get closer to the cylinder walls. The flame surface fraction which is close to the cylinder walls then increases, until the moment when the whole flame surface has spread inside the cylinder, vanishing into the walls (flame surface fraction equals to 1).

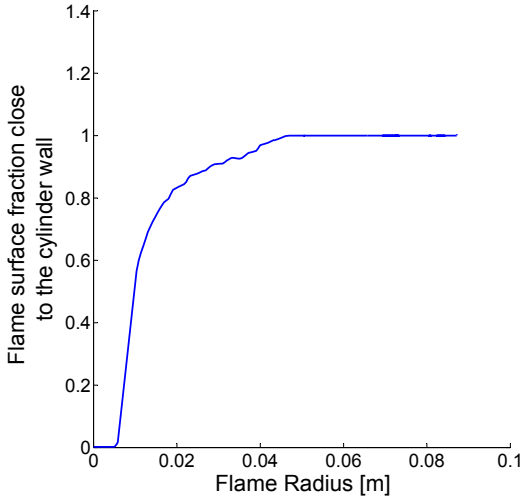

Figure 6: Flame Surface Fraction at a distance $d_i < L_i/2$ as a function of the flame radius

.

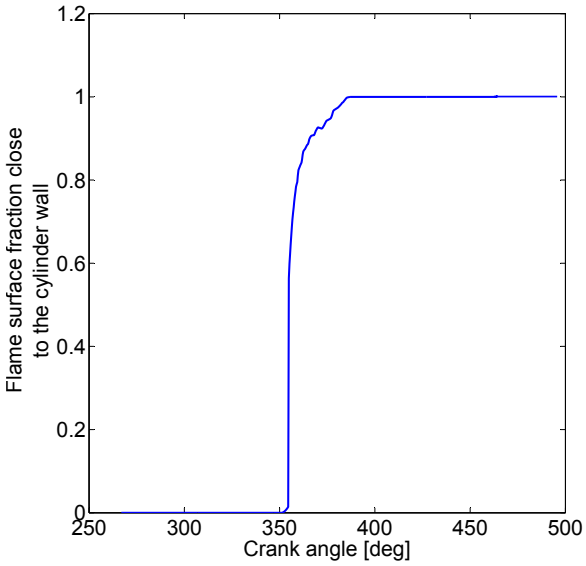

Figure 7: Flame surface fraction with respect to the crank angle during combustion for distances from the cylinder wall below $L_i/2$.

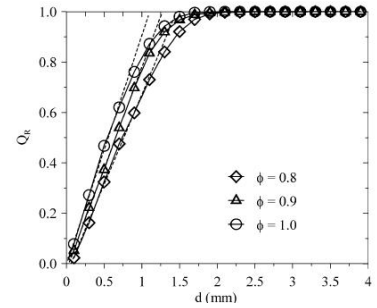

(a) Evolution of Q_R respect to the distance to the cylinder walls. [22]

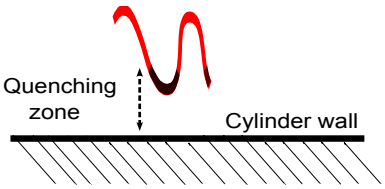

(b) Extinguishing zone

Figure 8: Linear deceleration of the burning rate close to the cylinder walls [22].

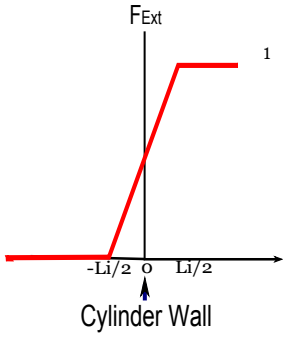

Figure 9: Extinction function F_{Ext}

Extinction function implementation

The extinction function is used to consider the influence of the cylinder walls while the flame surface is developing in the combustion chamber. It is defined as a function of the distance from the flame surface to the cylinder walls. For larger distances between the flame surface and the cylinder walls, the value of this function is assigned to one; it means that the flame surface is developing completely free in the combustion chamber, without attenuations in the burning rate.

When the flame is getting close to the cylinder walls, the flame surface can be considered as decreasing linearly as a function of the distance to the wall [22]. Figure 8 extracted from [22] supports this assumption. In this figure, in the graphic 8a Q_R is the ratio between the length of reactive flamelet (localized at a distance greater than the quenching zone, but in the vicinity of the piston where the flame is extinguished, Figure 8b), to the total flamelet length in the same vicinity and ϕ is the equivalence ratio [22].

In Figure 9, the designed extinction function is presented. It represents the flame surface behavior with respect to the wall interaction. For distances that reach $L_i/2$, there is a linear decrease, represented by the $1/L_i$ slope in the extinction function. When the distance to the cylinder walls is zero ($l = 0$), the function value is assigned to 0, representing the flame surface which has been extinguished (negative distance).

Flame/Wall Interaction sub model implementation

The extinction function is applied to the flame surface fraction in (24). The result is integrated across the distance to the cylinder wall up to $L_i/2$ as:

$$\Psi = \int_{l=-L_i/2}^{l=L_i/2} F_{Ext} A_{f_{d_i<L_i/2}} dl \tag{26}$$

The Figures 10, 11 and 12 show a scheme of the flame surface propagating inside the combustion chamber and the flame surface fraction distribution that corresponds to each piston height and flame radius lengths multiplied by the extinction function. In the figures, L_i is set to a constant value to give a simpler view of the process, but in the combustion model L_i varies with time. The original flame surface fraction and the extinction function are overlapped in the figure for a better understanding.

The results are stored in a map which represents the flame wall interaction when it approaches the cylinder walls, and is denoted by Ψ. Ψ depends on the flame radius, the piston height, and the integral scale. During the simulation, the values of the map are interpolated, resulting in a Ψ function that represents the deceleration of the burning rate depending on the flame surface distribution in the combustion chamber.

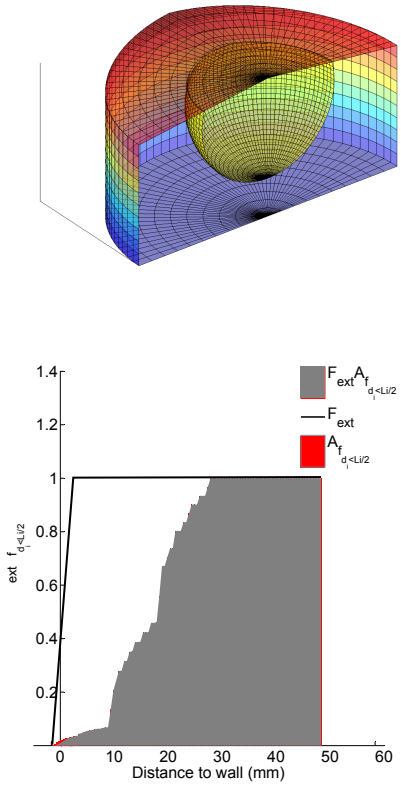

Figure 10: $R_f = 21\,mm$, $H_p = 40\,mm$, $L_i = 3\,mm$, $\Psi = 0.985$

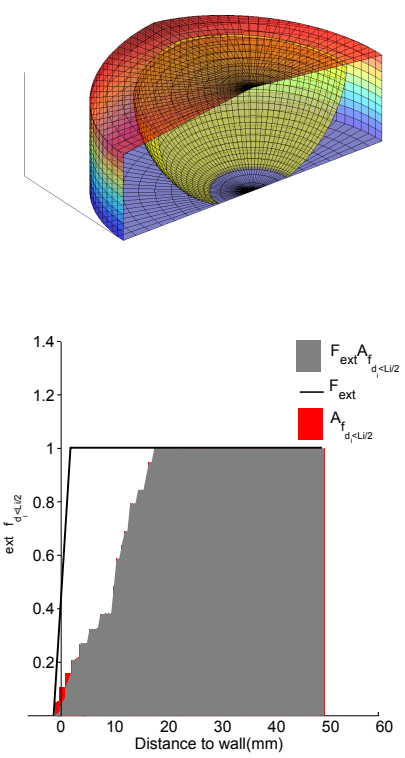

Figure 11: $R_f = 30\,mm$, $H_p = 30\,mm$, $L_i = 3\,mm$, $\Psi = 0.89$

Including the submodel Ψ in the burning rate equation, the proposed burning rate for the combustion model is represented by (23).

MODEL VALIDATION

The model was tested taking as reference the measurements on a 2 liters engine. Table 1 summarizes the main characteristics of the test engine. The data to fit the model are the pressure and the rate of energy released. The test was performed at $N = 5250\,rpm$, BMEP $= 11.4\,bar$. Figure 13 shows a resulting Ψ for a simulation when the chosen distance to have the walls influence is set to $L_i/2$ with $L_i = 0.05\sqrt[3]{V_{cyl}}$ according to [7]. At the beginning of combustion, Ψ is one because all the flame surface is propagating freely across the chamber. This means that the flame surface is not influenced by the walls (Ξ is weighted by $\Psi = 1$). Once the flame starts to get close to the walls, Ψ decreases because part of flame has already touched the walls, thus decreasing the burning rate. In the figure, Ψ exhibits a saw tooth behavior: at each computation step, Ψ is interpolated depending on the current flame surface that reaches a distance $d_i < L_i/2$ from the cylinder walls. If the free flame surface spreading in the combustion chamber is smaller than the flame surface lost in the barrier (i.e. the cylinder head), it might happen that the flame surface used to compute the flame surface fraction $A_{f_{d_i}}$ at the current step is smaller than the fraction computed in the previous step, then Ψ decreases for the current computation.

Displacement: 1998 cm3
Bore x Stroke: 82.7x93 mm
Number of cylinders: 4
Number of valves: 16
Volumetric ratio: 9.3:1
Max Rev: 6000 rpm
Min Rev: 1000 rpm

Table 1: Engine Test Characteristics

The main results are shown in Figure 14, where the comparison of the simulations when Ψ is included with respect to the first studied model are presented. In Figure 14b, the cylinder pressure has its maximum after the top center crank angle, but before the cylinder charge is fully burned. It coincides with the moment when the flame reaches the cylinder walls [9]. For this reason, when Ψ is not included in the system, the heat release rate shown in Figure 14a and the cylinder pressure in Figure 14b show an abrupt rise because the burning rate deceleration is not taken into account. Similarly, the cylinder pressure shows a bigger peak than expected when compared with the measurements. When Ψ is included, the heat release rate is reduced at the end of the combustion process

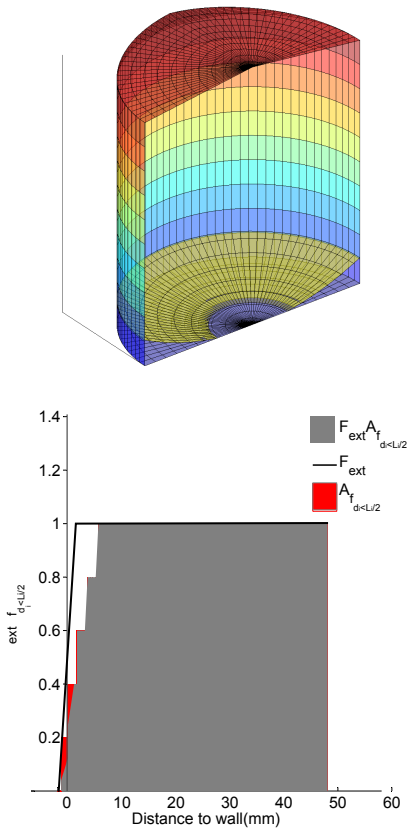

Figure 12: $R_f = 89\,mm$, $H_p = 90\,mm$, $L_i = 3\,mm$, $\Psi = 0.76$

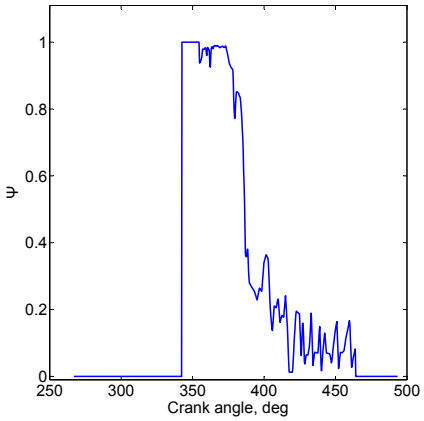

Figure 13: Evolution of Ψ during simulation.

because of the deceleration on the burning rate. As a consequence the peak on the cylinder pressure is equally reduced. It shows that the introduction of a deceleration on the burning rate is required before the cylinder charge is fully burned, which coincides with the moment when the flame reaches the cylinder walls.

Special care must be taken into account when analyzing the results under low load conditions. The figures 16 and 15 show two operating points at low load condition. These figures present a less accurate

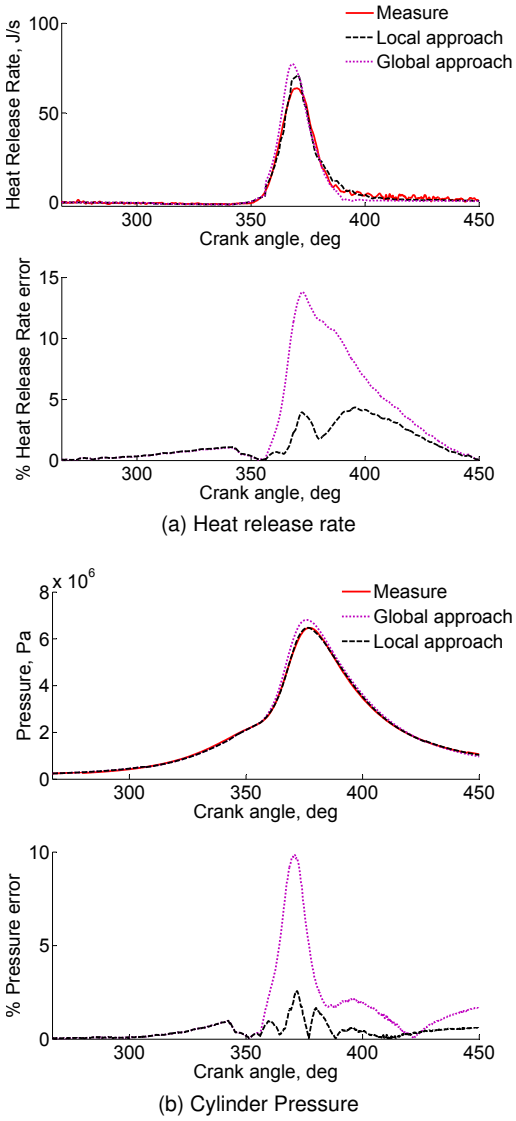

Figure 14: Heat release rate and cylinder pressure for the burning rate model (19)., BMEP = 11.4 bar, N = 5250 rpm.

behavior when compared with figure 14. In low load conditions, the cyclic variation of the engine tends to be greater than in high load operating conditions [27], this behavior alters the combustion process. To represent such behavior, an appropriate model of the cyclic variation can be included. In the case of this work, the cyclic variation is taken into account, however, it does not make part of the main subject of this work, therefor this topic is modeled in a basic way. For the reason mention previously, prudence is suggested when using the flame-walls interaction submodel under low load conditions.

Figure 18 shows an experience under low speed conditions ($N = 1000rpm$). The results are satisfactory, but prudence is required when interpreting those results. In [28], it is shown that while increasing engine speed, the characteristic wrinkling scale and the Kolmogorov scale decrease. Therefore, the time arrival of the flame surface to

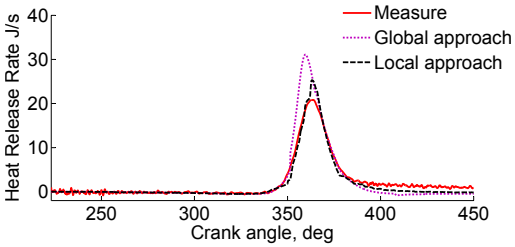

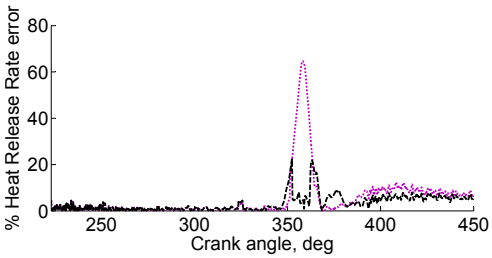

(a) Heat release rate

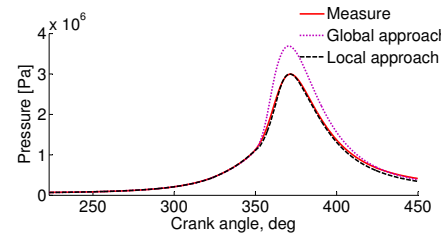

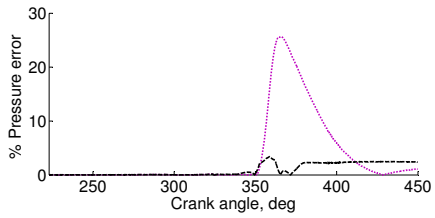

(b) Cylinder Pressure

Figure 15: Heat release rate and cylinder pressure for the burning rate model (19) BMEP=4.723 bar, N=4400rpm.

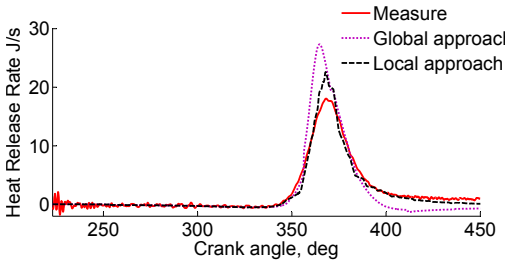

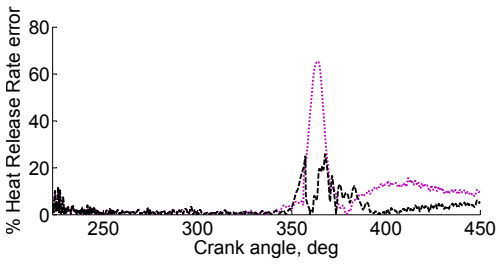

(a) Heat release rate

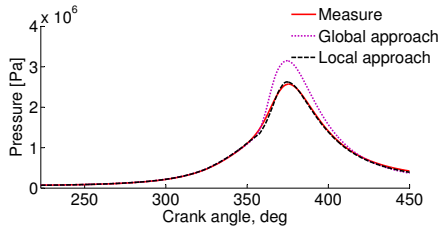

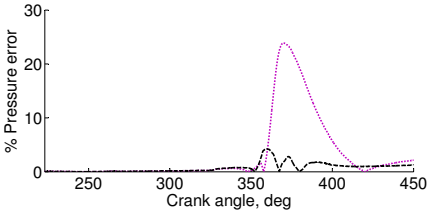

(b) Cylinder Pressure

Figure 16: Heat release rate and cylinder pressure for the burning rate model (19). BMEP=4.75 bar, N=4000rpm.

the wall becomes smaller, lowering the influence of the quenching phenomenon. Contrary, in low speed operating conditions, the quenching phenomena become more significant. In the case of this work, even if the quench model is based on an integral scale computed with a geometrical aspect, it is also related to the wrinkling phenomena via the flame radius. For this reason, the function Ψ might be used in low speed as well as in high speed operating conditions. For the submodel proposed in this work, a bigger integral scale in low operating conditions means a less steep slope on the extinction function presented earlier; giving a bigger deceleration of the burning rate, which would be the desired effect for low speed conditions. To be more coherent with the phenomena, a more accurate approximation of the integral scale taking into account the engine speed is recommended.

In the figures, the measures are presented in solid lines and the model results before and after the inclusion of Ψ are in dotted and dashed line, respectively. The errors on heat release rate and cylinder pressure are reduced approximatively by a factor of 3 thanks to the proposed local approach. Complementary results are shown in figures 15, 16 and 17.

CONCLUSIONS

A two zones combustion model has been implemented to model the combustion process in a S.I engine and the definition of a new submodel that models the impact of the cylinder walls in burning rate has been proposed. This new model takes into account the impact of the cylinder walls using to the flame surface distribution with respect to the combustion chamber and the assumed linear decay during the flame-wall interaction. A well-defined geometric model of the

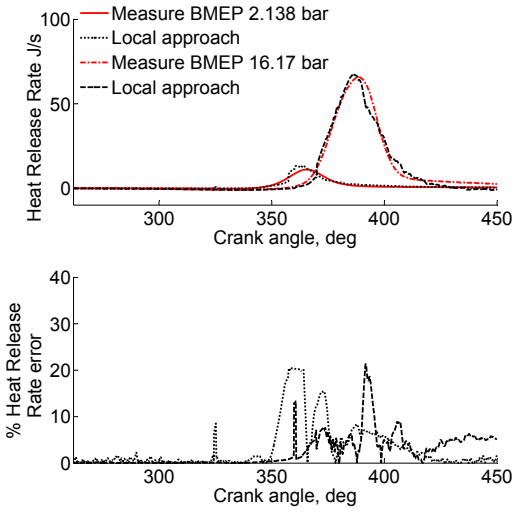

(a) Heat release rate

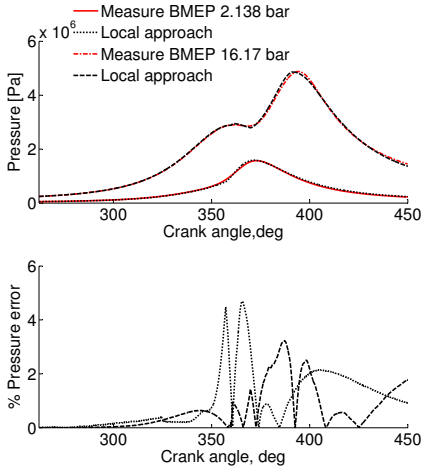

(b) Cylinder Pressure

Figure 17: Heat release rate and cylinder pressure for the burning rate model (19), N=1700rpm

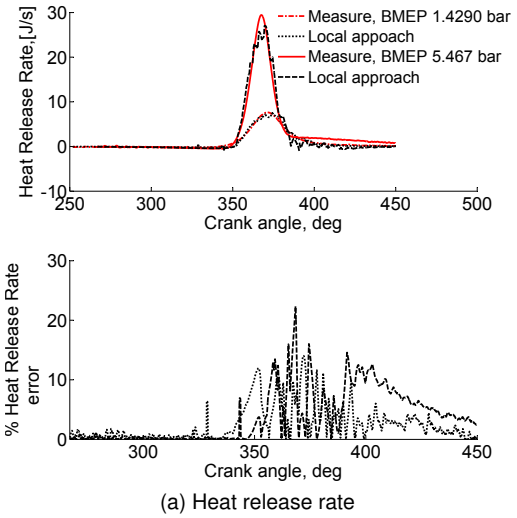

(a) Heat release rate

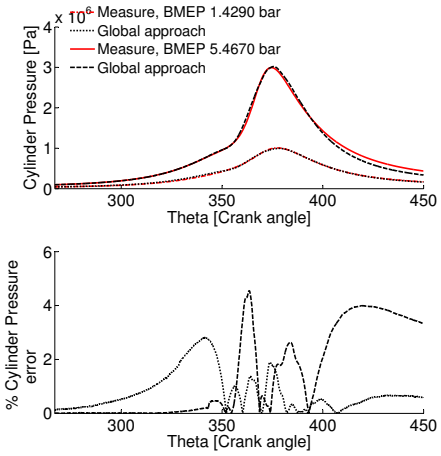

(b) Cylinder Pressure

Figure 18: Heat release rate and cylinder pressure for the burning rate model (19), N=1000rpm

combustion chamber has been designed in order to have more realistic results. The proposed model has been included in the 0D two zones combustion model and might be included in several combustion schemes as it is conceived as a dimensionless function multiplying the burning rate equation.

The model has been validated against experimental measurements on a 2 liter engine. When the flame-wall interaction is not well taken into account, the energy release is usually overestimated at the end of the combustion process, as well as the cylinder pressure. When the proposed flame-wall interaction model is included, very satisfying results are obtained; the model improves dramatically with an enhanced fit to the measurements when compared to less accurate approximations, in terms of heat release rate and cylinder pressure estimation.

REFERENCES

[1] A.Nefischer, J.Neuman, A.Stanciu, and A.Wimmer. Comparison and application of different phenomenological combustion models for turbo-charged SI engines. *SAE International Powertrains, Fuels and Lubricants Meeting 2010*, (2010-C-170), 2010.

[2] O.Colin, A.Benkenida, and A.Angelberger. 3D modeling of mixing, ignition and combustion phenomena in highly stratified gasoline engine. *Oil and Gas Science and Technology*, 58:47–62, 2003.

[3] S.Bougrine, S.Richard, and D.Veynante. Modelling and simulation of the combustion ethanol blended fuels in a SI engine using a 0D coherent flame model. *SAE International*, (2009-24-0016), 2009.

[4] S.Yoshiyama, E.Tomita, Z.Zhang, and Y.Hamamoto. Measurements and simulation of turbulent flame propagation in a spark ignition

engine by using fractal burning model. *SAE*, (2001-01-3603), 2001.

[5] F.Bozza, A.Gimelli, S.Merola, and B.Vaglieco. Validation of a fractal combusition model through flame imaging. *Modeling of SI and Diesel Engines 2005*, (2005-01-1120), 2005.

[6] M.Baratta, A Catania, E.Spessa, and A.Vassallo. Development of an improved fractal model for the simulation of turbulent flame propagation in SI engines. *SAE*, (2005-24-082), 2005.

[7] F.Bozza, A.Gimelli, L.Strazzullo, E.Torella, and C.Cascone. Steady state and transient operation simulation of a downsized turbocharged SI engine. *Modeling of SI and Diesel Engines*, (2007-01-0381), 2007.

[8] P.Pierce, J.Ghandhi, and J.Martin. Near-wall velocity characteristics in valved and ported motored engines. *SAE*, (920152), 1992.

[9] J.Heywood. *Internal Combustion Engine Fundamentals*. McGraw-Hill International Editions, 1988.

[10] M.Chase Jr, C.Davies, J.Downey Jr, D.Frurip, and R.McDonald. *JANAF Thermochemical Tables*. American Institute of Physics, 3rd edition, 1986.

[11] N.Bordet, C.Caillol, P.Higelin, and V.Talon. A physical 0D combustion model using tabulated chemistry with presumed probability density function approach for multi injection diesel engines. (2010-01-1493), 2010.

[12] G.Woschni. A universally applicable equation for the instantaneus heat transfer coefficient in the interal combustion engine. (670931), 1967.

[13] X.Zhao, R.Matthews, and E.Ellzey. Numerical simulations of combustion in SI engines: Comparison of the fractal flame model to the coherent flame model. *International Symposium COMODIA*, 1994.

[14] M.Ulinski, P.Moore, M.Elia, and M.Metghalchi. Laminar burning velocity of methane air diluent mixtures. 1980.

[15] L.Gulder. Correlations of laminar combustion data for alternative si engine fuels. *SAE*, (841000), 1984.

[16] L.Gulder, G.Smallwood, R.Wong, D.Snelling, and R.Smith. Flame front surface characteristics in turbulent premixed propane/air combustion. *Combustion and Flame*, 120:407–416, 2000.

[17] F.Lafossas, O.Colin, F.Le Berr, and P.Menegazzi. Application of a new 1D combustion model to gasoline transient engine operation. (2005-01-2107), 2005.

[18] T.Poinsot and D.Veynante. *Theroetical and numerical combustion*. Edwards, 2001.

[19] H.Weller, S.Uslu, A.Gosman, R.Maly, R.Herweg, and B.Heel. Prediction of combustion in homogeneus charge spark ignition engines. *Internationl Symposium COMODIA*, 1994.

[20] K.Nishaiwaki and K.Saijyo. Modeling of flame wall interaciton in SI engine combustion. *Proceedings of the 15 Internal Combusiton Engine Symposium*, (9935158):63–68, 1999.

[21] T.Kojima and K.Nishiwaki. Modelling of flame wall interaction for combustion and heat transfer in SI engines. *JSAE Review*, 18:11–17, 1996.

[22] F.Foucher and C.Mounaim-Rousselle. Fractal approach to the evaluation of burning rates in the vecinity of the piston in a spark-ignition engine. *Combustion and Flame*, 143:323–332, 2005.

[23] D.Wilcox. *Turbulence modeling for CFD*. DCW Industries, 1993.

[24] G.Valentino, F.Corcione, and G.Seccia. Integral and micro time scales estimate in DI diesel engines. *International spring fuels & lubricants meeting*, (971678), 1997.

[25] D.Boggs and G.Borman. Calculation of heat flux integral length scales from spatially-resolved surface temperature measurements in an engine. *International Congress and Exposition*, (910721), 1991.

[26] O.Kaario, M.Larmi, and F.Tanner. Relating integral length scale to turbulent time scale and comparing k-e and rng k-e turbulence models in diesel combustion simulation. *Modeling of SI Engines and Multi Dimensional Engine Modeling*, (2002-01-1117), 2002.

[27] G.A Karim, R.R Raine, and W.Jones. An examination of cyclic variations in a dual fuel engine. *SAE International Fall Fuels and Lubricants Meeting and Exhibition*, (881661), 1988.

[28] T.Steiner and K.Boulouchos. Near-wall unsteady premixed flame propagation in SI engines. *International Congress and Exposition SAE*, (951001), 1995.

[29] F.Alizon. Transferts de chaleur convectifs dans la chambre de combustion des moteurs à combustion interne: Influence de l'arodynamique interne. Technical report, PARIS VI, 2005.

[30] H.Tennekes and J.Lumley. *First course in turbulence*. The MIT press, 1985.

[31] C.Barba and C.Burkhardt. A phenomenological combustion model for heat release rate prediction in hith-speed DI diesel engines with common rail injection. *SAE*, 2000.

[32] S.Richard, S.Bougrine, G.Font, F.Lafossas, and F.Le Ber. On the reduction of a 3D CFD combustion model to build a physical 0D model for simulating heat release, knock and pollutants in si engines. *Oil and Gas Sciend and Technology*, 64:223–242, 2009.

ACKNOWLEDGMENTS

The authors wish to thank to Julien Parodi for his technical contributions.

APPENDIX

0D PHENOMENOLOGICAL $k-\epsilon$ TURBULENCE MODEL

The turbulence model defines the eddies characteristics of the turbulent flow field. Thanks to the turbulence model, the turbulence intensity u' and the integral scale L_i are defined. These variables have an important impact in the SI model and in the flame/wall interaction modeling.

This turbulence model is based on the *Reynolds stress tensor* τ, where the kinetic energy per unit volume of the turbulence fluctuations is assumed to be proportional to the trace of the *Reynolds stress tensor* equation [23]. The dynamics of τ is given as:

$$\begin{aligned}&\frac{\partial \tau_{ij}}{\partial t} + U_k \frac{\partial \tau_{ij}}{\partial x_k} = -\tau_{ik}\frac{\partial U_j}{\partial x_k} - \tau_{ij}\frac{\partial U_i}{\partial x_k} + \epsilon_{ij} \\ &- \pi_{ij} + \frac{\partial}{\partial x_k}\left(v\frac{\partial \tau_{ij}}{\partial x_k} + C_{ijk}\right)\end{aligned} \tag{27}$$

$$\pi_{ij} = \overline{p\left(\frac{\partial u_i}{\partial x_j} + \frac{\partial u_j}{\partial x_i}\right)} \tag{28}$$

$$\epsilon = \overline{2\mu \frac{\partial u_i}{\partial x_k}\frac{\partial u_j}{\partial x_k}} \tag{29}$$

$$C_{ijk} = \overline{\rho u_i u_j u_k} + \overline{pu}\delta_{jk} + \overline{puj}\delta_{ik} \tag{30}$$

where u is the fluid velocity, U is the mean fluid velocity, π_{ij} is the pressure strain correlation tensor, ϵ is the dissipation rate and C_{ijk} is the turbulent transport tensor. (Notice that in the appendix, U makes reference to a velocity, contrary to the other sections of the article where U makes reference to internal energy).

The Reynolds-stress tensor describes the random fluctuations of the various flow properties. According to Reynolds, all the quantities are expressed as sums of mean fluctuating parts. These equations are too complex for the purpose of this work, and will not be explained in details. They are exposed here in order to show the reference for the 0D turbulent energy model used in the qualitative analysis results and various dependencies.

Reynolds stress tensor equation 0D reduction

The model reduction is based on the work developed in [29]. The kinetic energy per unit mass is defined according to Prandlt as:

$$k = \frac{1}{2}\overline{u_i u_i} \tag{31}$$

Based on the the Reynolds stress tensor, it is possible to derive the corresponding dynamics for k. The tensor (28) vanishes for incompressible flows. Rearranging the equation (27) under the assumption (31), the following transport equation for the turbulent kinetic energy is obtained [30]:

$$\begin{aligned}&\frac{\partial k}{\partial t} + \overline{U_j}\frac{\partial k}{\partial x_j} = -\overline{u_i u_j}\frac{\partial \overline{U_i}}{\partial x_j} \\ &- \frac{\partial}{\partial x_j}\overline{\left(\left(\frac{P_{cyl}}{\rho} + \frac{1}{2}u_i u_i\right)u_j\right)} \\ &+ v\frac{\partial^2 k}{\partial x_j x_j} - v\overline{\frac{\partial u_i}{\partial x_j}\frac{\partial u_i}{\partial x_j}}\end{aligned} \tag{32}$$

The left hand side of the equation (32) is due to the convection phenomenon. On the right hand, the first term corresponds to the turbulent energy production term, the second term is the turbulent diffusion, the third term is the diffusion due to molecular agitation and the last term is the isotropic dissipation. The speed U_i in the direction i is defined as the sum of the mean speed $\overline{U_i}$ and a fluctuation u_i:

$$U_i = \overline{U_i} + u_i \tag{33}$$

The turbulent diffusion term is modeled as:

$$-\frac{\partial}{\partial x_j}\overline{\left(\left(\frac{P_{cyl}}{\rho} + \frac{1}{2}u_i u_i\right)u_j\right)} = \frac{\partial}{\partial x_j}\left(\frac{v_{Turb}}{\sigma_k}\frac{\partial k}{\partial x_j}\right) \tag{34}$$

where v_{Turb} is the thermal diffusivity and σ_k is a constant. The dissipation is based on the Prandtl-Kolmogorov hypothesis:

$$\epsilon = v\overline{\frac{\partial u_i}{\partial x_j}\frac{\partial u_i}{\partial x_j}} = C_{diss}\frac{k^{3/2}}{L_i} \tag{35}$$

where C_{diss} is a calibration constant fixed to 0.04. Including (34) and (35) in equation (32), follows that:

$$\frac{\partial k}{\partial t} + \overline{U_j}\frac{\partial k}{\partial x_j} = -\overline{u_i u_j}\frac{\partial \overline{U_i}}{\partial x_j} + \frac{\partial}{\partial x_j}\left(\frac{v_{Turb}}{\sigma_k}\frac{\partial k}{\partial x_j}\right) + v\frac{\partial^2 k}{\partial x_j x_j} - C_{diss}\frac{k^{3/2}}{L_i} \quad (36)$$

The turbulent kinetic energy k is supposed to be homogeneous in the combustion chamber according to [31]: it implies that k is constant with respect to the spatial coordinates. Under this assumption $\frac{\partial k}{\partial x_j} = 0$ and (36) is reduced to:

$$\frac{\partial k}{\partial t} = -\overline{u_i u_j}\frac{\partial \overline{U_i}}{\partial x_j} - C_{diss}\frac{k^{3/2}}{L_i} \quad (37)$$

In order to obtain a 0D expression, the last term to define is the production term. This term can be defined as a function of the spatial speed taking apart the isentropic ($i = j$) and non-isentropic ($i \neq j$) parts. For the isentropic part:

$$\overline{u_i u_j}\frac{\partial \overline{U_i}}{\partial x_j}_{i=j} = \overline{u_1 u_1}\frac{\partial \overline{U_1}}{\partial x} + \overline{u_2 u_2}\frac{\partial \overline{U_2}}{\partial y} + \overline{u_3 u_3}\frac{\partial \overline{U_3}}{\partial z} \quad (38)$$

From equation (31), for the isentropic case, $\overline{u_1 u_1} = \overline{u_2 u_2} = \overline{u_3 u_3} = \frac{2}{3}k$. Including this equality in (38) the final expression for the production term is obtained as:

$$\overline{u_i u_j}\frac{\partial \overline{U_i}}{\partial x_j} = \frac{2}{3}k\nabla\mathbf{U} + \overline{u_i u_j}\frac{\partial \overline{U_i}}{\partial x_j}_{non-isentropic} \quad (39)$$

where **U** is $(\overline{U_1}, \overline{U_2}, \overline{U_3})$.

Taking the continuity equation for fluids and assuming that the density ρ is constant over the space:

$$\frac{\partial \rho}{\partial t} + \rho\nabla\mathbf{U} = 0 \quad (40)$$

It is also assumed that the density is constant (incompressible gas), then the speed **U** divergence is also 0. Including this result in (37), the production term is only related to the non-isentropic speed as:

$$\frac{\partial k}{\partial t} = -\overline{u_i u_j}\frac{\partial \overline{U_i}}{\partial x_j}_{non-isentropic} - C_{diss}\frac{k^{3/2}}{L_i} \quad (41)$$

The non-isentropic production term represents the turbulent kinetic energy produced by the different turbulent sources: the swirl, the squish, the spray and the tumble. For a SI engine, the effects of swirl, squish and spray on turbulence can be neglected [17]. The tumble energy is then the only turbulence source for the production term:

$$-\overline{u_i u_j}\frac{\partial \overline{U_i}}{\partial x_j}_{non-isentropic} = \frac{\partial k}{\partial t}_{tumble} \quad (42)$$

The turbulent kinetic energy due to the tumble can be obtained assuming a linear decrease of the tumble motion from the intake valve closure (IVC) to the top dead center as it is suggested in [32]:

$$\frac{\partial k}{\partial t}_{tumble} = \frac{1}{8}m\omega_{eng}^2\left(L^2\frac{dN_{tumble}}{dt} + 2N_{tumble}L\frac{dL}{dt}\right) \quad (43)$$

where L is the piston height, ω_{eng} is the engine speed in rad/s and N_{tumble} is the tumble number.

The computation of the tumble number N_{tumble} can be complex. For the purpose of this work it is concluded that a data map of the initial tumble number would be used.

Including (42) in (41) the turbulent kinetic energy is obtained as:

$$\frac{\partial k}{\partial t} = \frac{1}{8}m\omega_{eng}^2\left(L^2\frac{dN_{tumble}}{dt} + 2N_{tumble}L\frac{dL}{dt}\right) - C_{diss}\frac{k^{3/2}}{l_i} \quad (44)$$

NOMENCLATURE

All variables are in S.I Metric Units.

A_f Flame surface fraction
A_l Laminar flame surface
A_t Turbulent flame surface
A_w Heat transfer wall area
C_L Calibration constant
c_p Specific heat at constant pressure
c_r Calibration constant
c_v Specific heat at constant volume
F_{Ext} Extinction function
h Enthalpy
h_c Heat transfer coefficient for wall looses
H_p Piston height
L_i Integral scale
L_k Kolmogorov scale

m Total mass in the combustion chamber
m_b Burned mass
m_f Fuel mass
m_u Fresh mass
p Pressure
Q Heat
r Specific gases constant
R_{cyl} Cylinder radius
R_f Flame radius
S_t Turbulent flame speed
S_l Laminar flame speed
T Temperature
u Internal energy
U Energy
V_{cyl} Cylinder volume
V_b Burned gases volume
V_u unburned gases volume
Y Species mass fraction
Ψ 0D submodel to take into account the impact of the walls in the burning rate
ρ_u Unburned gas density
Ξ Wrinkling coefficient
γ Specific heat ratio
X_{egr} Exhaust gas recirculation fraction
ϕ Air to fuel ratio